Nanoscale

Accepted Manuscript

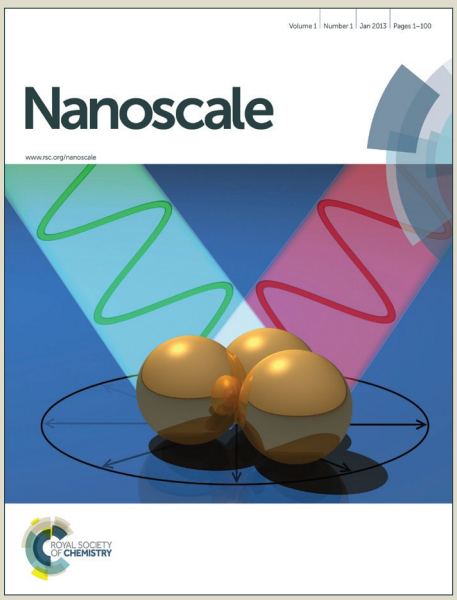

ROYAL SOCIETY OF CHEMISTRY

www.rsc.org/nanoscale

Nanoscale

COMMUNICATION

Cite this: DOI: 10.1039/xxxxxxxxxx

Targeted silver nanoparticles for ratiometric cell phenotyping†

Anne-Mari A. Willmore,[a] Lorena Simón-Gracia,[a] Kadri Toome,[a] Päärn Paiste,[b] Venkata Ramana Kotamraju,[c] Tarmo Mölder,[a] Kazuki N. Sugahara,[‡c] Erkki Ruoslahti, [cd] Gary B. Braun,[*c] and Tambet Teesalu[*acd]

Received Date
Accepted Date

DOI: 10.1039/xxxxxxxxxx

www.rsc.org/journalname

Affinity targeting is used to deliver nanoparticles to cells and tissues. For efficient targeting, it is critical to consider the expression and accessibility of the relevant receptors in the target cells. Here, we describe isotopically barcoded silver nanoparticles (AgNPs) as a tool for auditing affinity ligand receptors in cells. Tumor penetrating peptide RPARPAR (receptor: NRP-1) and tumor homing peptide GKRK (receptor: p32) were used as affinity ligands on the AgNPs. The binding and uptake of the peptide-functionalized AgNPs by cultured PPC-1 prostate cancer and M21 melanoma cells was dependent on the cell surface expression of the cognate peptide receptors. Barcoded peptide-functionalized AgNPs were synthesized from silver and palladium isotopes. The cells were incubated with a cocktail of the barcoded nanoparticles [RPARPAR (R), GKRK (K), and control], and cellular binding and internalization of each type of nanoparticle was assessed by inductively coupled plasma mass spectrometry. The results of isotopic analysis were in agreement with data obtained using optical methods. Using ratiometric measurements, we were able to classify the PPC-1 cell line as mainly NRP-1-positive, with 75 ± 5% R-AgNP uptake, and the M21 cell line as only p32-positive, with 89 ± 9% K-AgNP uptake. The isotopically barcoded multiplexed AgNPs are useful as an *in vitro* ratiometric phenotyping tool and have potential uses in functional evaluation of the expression of accessible homing peptide receptors *in vivo*.

1 Introduction

Nanoparticles (NPs) are widely used as cancer drug delivery vehicles to increase drug efficacy and decrease off-target effects [1–4]. NPs can be rendered tumor-selective by active targeting with affinity ligands, such as antibodies and homing peptides [5,6]. Tumor homing peptides identified using *in vivo* phage display are particularly well suited for the targeting of NPs, because the phage particles used to display exogenous peptides during the screening are biological nanoparticles and because multivalent presentation on NPs augments target binding through an avidity ("velcro") effect. Recently, we used *in vivo* phage display to identify a novel class of tumor targeting peptides that extravasate and penetrate into tumor parenchyma using a C-terminal R/KXXR/K sequence ("C-end Rule" or CendR motif) [7,8]. The CendR motif binds to cell surface neuropilin-1 (NRP-1), a cell surface pleiotropic hub receptor with essential roles in vascular biology that is overexpressed in angiogenic endothelial cells, tumor cells, and cells in tumor stroma [9]. Many cultured cancer cells, such as PC-3 and PPC-1 prostate cancer cells [7,10], overexpress NRP-1. RPARPAR is a prototypic CendR peptide that binds to and internalizes into cells that express NRP-1 [7]. Another tumor homing peptide identified by *in vivo* phage display, CGKRK, homes to tumors by a mechanism that involves p32 protein – a mitochondrial chaperone that is aberrantly expressed at the cell surface in activated cells such as tumor blood and lymphatic endothelial cells, tumor cells, and tumor macrophages [11–13]. High p32 expression correlates with poor prognosis in prostate cancer patients [14]. CGKRK has been used to deliver compounds to transgenic squa-

[a] *Laboratory of Cancer Biology, Institute of Biomedicine, Centre of Excellence for Translational Medicine, University of Tartu, Ravila 14B, Tartu, 50411, Estonia. Tel: +372-53974441 E-mail: tambet.teesalu@ut.ee*

[b] *Department of Geology, University of Tartu, Ravila 14A, Tartu, 50411, Estonia.*

[c] *Sanford Burnham Prebys Medical Discovery Institute, Cancer Research Center, 10901 N. Torrey Pines Road, La Jolla, CA, 92037 USA. Tel: (858) 646-3100 E-mail: gbraun@sbpdiscovery.org*

‡ Present Address: Department of Surgery, Columbia University College of Physicians and Surgeons, New York, NY, USA

[d] *Center for Nanomedicine, and Department of Molecular Cellular and Developmental Biology, University of California, Santa Barbara, Santa Barbara, CA, USA*

† Electronic Supplementary Information (ESI) available: [TEM images of isotopic AgNPs, cell antibody staining, coadministration ICP-MS data, and biotin control particle ICP-MS data]. See DOI: 10.1039/b000000x/

mous cell carcinoma (K14-HPV16) lesions, and to glioblastoma and breast cancer xenografts in mice [11,12,15].

Recently, we developed a silver nanoparticle (AgNP) platform for cell internalization and tissue penetration studies [16]. The AgNPs can be functionalized with tumor homing peptides and other affinity ligands for *in vitro* and for *in vivo* targeting. AgNPs surface-labeled with a fluorophore are very bright because the NPs greatly enhance the fluorescence intensity due to plasmonic effect. Moreover, extracellular AgNPs can be "etched," or dissolved, using a mild biocompatible solution to differentiate between internalized and surface-bound exposed particles [16].

Here we present advancement to the AgNP platform: isotopic multiplexing. We show that a cocktail of isotopically-tagged AgNPs, each conjugated with a different homing peptide, can be used in multiplex to map the expression status of more than one homing peptide receptor simultaneously. Applied to an *in vivo* situation, this ratiometric phenotyping system will allow quantitative and internally controlled evaluation of accessible homing peptide receptor expression in target tissues.

2 Methods

Materials

$AgNO_3$ wt (Sigma-Aldrich #209139); $AgNO_3$ 107Ag and 109Ag >99% pure isotopes (Isoflex); sodium citrate tribasic dihydrate (Sigma-Aldrich #S4641); tannic acid (Sigma-Aldrich #403040); D-biotin (Sigma-Aldrich #B4501); $Pd(NO_3)_2$ (Aldrich #76070); NeutrAvidin (Thermo Scientific #31055); Lipoic acid-PEG(1k)-NHS (Nanocs #PG2-AMLA-1k); CF555-NHS dye (Biotium #92130); HNO_3 (Fluka #84385); HCl (Fluka #84415); NH_4OH (Fluka #09857); Peptides were synthesized in-house at SBPMDI or ordered from TAG Copenhagen.

AgNP Synthesis

Particle synthesis was done by modified Lee and Meisel citrate method [17,18]. In the dark, 50.4 mg of $AgNO_3$ was dissolved in 1 mL of Milli-Q water (MQ, resistivity 18 MΩ-cm) and added to a piranha-cleaned (H_2SO_4 and H_2O_2 cleaned; *Caution: highly oxidizing acid solution*) flask containing 500 mL of water already heated to 65 °C. 1.2 mg of tannic acid was dissolved in 10 mL of MQ and 200 mg of citrate tribasic dihydrate was added to the solution. This mixture was added to the $AgNO_3$ solution in the reaction vessel. The mixture was vigorously stirred with a temperature of approximately 70 °C. The reaction was allowed to proceed for 3 min, at which point the solution turned yellow. The flask was then transferred to a pre-heated hot-plate, brought to a boil, and boiled for 20 min. Then the heat was turned off and the flask was left to cool to room temperature. The boiled-off volume of water was replaced with fresh MQ to bring back up to 500 mL. For the 1% Pd particles the same procedure was followed except 49.9 mg of $AgNO_3$ and 0.8 mg of $Pd(NO_3)_2$ were dissolved in water and mixed, then added to the reaction vessel.

AgNP Functionalization

The particles were functionalized, as previously described [16], with NeutrAvidins (NA) for biotinylated-peptide conjugation, and with Lipoic acid-polyethylene glycol(1k)-NH_2 (PEG) molecules. The PEG's terminal amines were used for dye coupling using CF555-N-hydroxysuccinimide-dye (NHS-dye). Three different particles were made by attaching biotinylated peptides: biotin-X-RPARPAR or biotin-X-SGKRK-NH_2 (X = aminohexanoic acid), or by blocking the biotin binding pocket with free D-biotin. Centrifuging at 21000 x*g*, decanting, and resuspension in fresh buffer (0.1 M HEPES pH 7.2, 0.1 M $NaNO_3$, 0.005% Tween 20) was used to wash away excess peptide.

Protein binding

His-tagged NRP-1 b1b2 domain (wt and mutant) were expressed and purified as described [7]. 6x-His-Tagged p32 was expressed in Rosetta-gami-2 cells (Novagen). The protein was purified by IMAC using HIS-select resin (Sigma) with an imidizole gradient from 20–300 mM and eluted fractions were analyzed on analytical SDS-PAGE. Sedimentation velocity assay was used to confirm the trimeric state of the recombinant p32 protein. AgNP binding experiments to magnetic beads coated with recombinant proteins were carried out with wtAgNPs. Ni-NTA magnetic agarose beads (Qiagen) in Tris buffer (50 mM Tris pH 7.4, 150 mM NaCl, 0.05% NP40, 5 mM imidazole) were loaded, as suggested by the manufacturer, with either the b1b2 binding domain of NRP1, with p32, or with a b1b2 mutant, followed by multiple washes. NPs were incubated for one hour with the protein loaded beads in Tris buffer with 1% BSA at room temperature with gentle agitation, followed by washes, and elution with high imidazole concentration buffer (PBS, 400 mM imidazole, 150 mM NaCl, 1% BSA, 0.05% NP40). The eluted samples were analyzed by UV-vis (NanoDrop 2000c, Thermo Scientific). The spectrum and maximum absorbance at 400 nm were recorded for each sample.

Cell Experiments

M21 and PPC-1 cells were grown in DMEM high glucose medium (PAA) with added serum, penicillin, and streptomycin (each from Gibco). For experiments, the medium was aspirated, the cells were washed twice with warm medium, and fresh medium was added along with NPs at 0.2 nM. The cells were incubated with NPs at 37 °C for one hour.

Microscopy

Microscopy experiments were carried out with wtAgNPs with CF555 dye. After incubation with AgNPs the NP containing medium was aspirated, the cells were washed, then fixed with -20 °C methanol, and washed with PBS. The cells were blocked (PBS, 1% BSA, 0.05% Tween-20) for 30 minutes at RT followed by primary NRP-1 and p32 antibodies for one hour at RT. The cells were washed and secondary antibodies (AF488-anti-mouse and AF647-anti-rabbit) were applied for 30 minutes at RT in the dark. Nuclei were stained with DAPI at 1 μg/mL. The coverslips were mounted onto glass slides with Fluoromount-G (Electron Microscopy Sciences) imaged using a Zeiss LSM710 confocal microscope.

Flow Cytometry

For flow cytometry experiments, AgNPs were labeled with the fluorescent dye CF555. The AgNPs were tested individually for binding against two cancer cell lines: PPC-1 and M21. After AgNP incubation, the AgNP containing medium was aspirated, the cells were washed with PBS, and dissociated from the culture dish with non-enzymatic Cell Dissociation Buffer (Gibco), transferred to 1.5 mL tubes, centrifuged, and suspended in 300 μL of PBS for analysis. The cells were analyzed for AgNP uptake with a BD Accuri flow cytometer by monitoring the 555 channel: FL2.

Etching

Etching solution was prepared fresh before each use from 0.2 M stock solutions of $Na_2S_2O_3$ and $K_3Fe(CN)_6$ stored in the dark. A working solution, 10 mM in each component diluted in PBS, was applied to cells for five minutes followed by PBS washes. *Warning! Do not dissolve $K_3Fe(CN)_6$ in concentrated acid solutions, as toxic HCN gas can be produced.*

ICP-MS experiments

Three atomically distinct particles: 107Ag, 109Ag, wtAg-Pd were used. After cell incubation with AgNPs, the medium was aspirated, cells washed with either PBS or etch solution, dissociated using non-enzymatic Cell Dissociation Buffer (Gibco), suspended and transferred to 1.5 mL tubes. The cells were spun down, aspirated, and then disrupted with 100 μL of 2% SDS solution. The samples were sonicated and transferred to glass vials and then treated with TraceSelect grade chemicals: 53 μL of HNO_3 and 160 μL of HCl to dissolve the AgNPs, slowly neutralized with 933 μL NH_4OH, diluted with MQ water and 0.22 μm filtered. The samples were analyzed using an Agilent 8800 QQQ ICP-MS.

Quantitation of the barcoded AgNPs

The quantity of wtAg-Pd particles was calculated based on measurement of the 105 isotope of Pd, and using that quantity to determine b-AgNPs' contribution to the 107Ag and 109Ag signals (brackets indicate concentration of analyte in ng/g):

$$[107]_{biotin} = 51.3 * [Pd] \quad (1)$$

$$[109]_{biotin} = 47.7 * [Pd] \quad (2)$$

$$\text{Total biotin} = [Pd] + [107]_{biotin} + [109]_{biotin} = 100 * [Pd] \quad (3)$$

$$\text{Total RPARPAR} = [107]_{total} - [107]_{biotin} \quad (4)$$

$$\text{Total SGKRK} = [109]_{total} - [109]_{biotin} \quad (5)$$

There is about 50x less palladium than of either of the two silver isotopes, therefore its detection by ICP-MS is less sensitive. This in itself may not be a problem because ICP-MS has a very good detection limit (as low as 10 pg/g for Ag and Pd); however, any error in the Pd measurement will be magnified 100-fold by the above calculations. Silver has only two stable isotopes and we used Pd-doped particles to allow multiplexing. The downside of particle doping is that it leads to an overlap in isotope signals which must later be deconvoluted. One way to avoid overlapping isotope signals would be to make all three, or more, particles doped with one of the six stable isotopes of Pd [19]. These doped particles would produce equally sensitive, yet distinguishable Pd signals with no overlap and no need for deconvolution calculations. In addition, duplex barcoding with just 107Ag and 109Ag, with one type of AgNP acting as an internal reference, provides a robust homing peptide evaluation and target phenotyping tool. This system can be deployed to assess the effect of homing peptide functionalization both *in vitro* for AgNP binding and internalization studies, and *in vivo* for biodistribution and pharmacokinetics analyses. Isotopically barcoded neutravidin AgNPs can be readily functionalized with biotinylated-peptides for auditioning of candidate peptides.

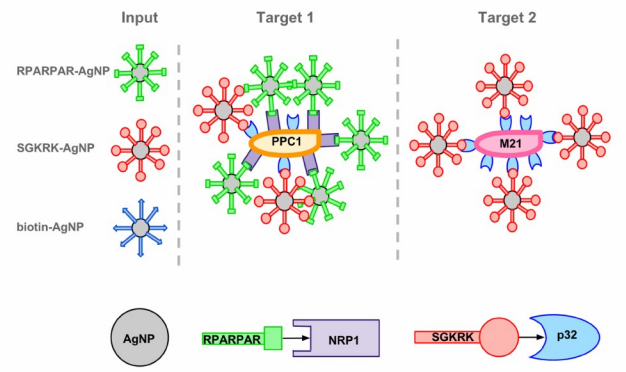

Fig. 1 Multiplexed ratiometric AgNP test system. The triplex system shown here is based on two targeting peptides: RPARPAR and SGKRK, and two biological targets: NRP-1 and p32. M21 cells express cell surface p32, whereas PPC-1 cells express both p32 and NRP-1 on the cell surface. Control biotin-AgNPs do not bind to either cell line and serve as a negative control. When an input of three different AgNPs is applied to the cells, their cell binding and uptake pattern will correlate with accessible cell surface receptor expression.

3 Results and Discussion

Our goal was to establish an isotopically-barcoded AgNP-based system for receptor phenotyping of cells using homing peptides (Figure 1). We used a modified citrate method to synthesize isotopically-barcoded AgNPs with a particle size of 24 $\pm$ 5 nm (Supp. Figure 1) [17,18]. For multiplexing, AgNPs were synthesized from >99% pure silver isotopes (107Ag or 109Ag), or from naturally occurring wild-type silver (wtAg), made up of 51.8% 107Ag and 48.2% 109Ag isotopes [19], with 1% Pd (wtAg-Pd). Each of the AgNP core types was neutravidin-coated and PEGylated, followed by functionalization with biotinylated peptides RPARPAR-OH (R) or SGKRK-NH2 (K), or biotin (B) as a negative control. SGKRK was used rather than CGKRK because replacing the cysteine with a serine avoids potential peptide-dimer formation. Cysteine is not required for the functionality of the peptide on nanoparticles [11].

The binding profile of wild-type R-AgNPs was evaluated by studying interaction with immobilized NRP-1 b1b2 and p32 recombinant proteins (Figure 2). As expected, R-AgNPs bound to wild-type NRP-1 b1b2 domain protein, but not to b1b2 protein with a mutated CendR binding pocket [7], or to p32 protein. K-AgNPs bound to immobilized p32, the main cellular receptor for

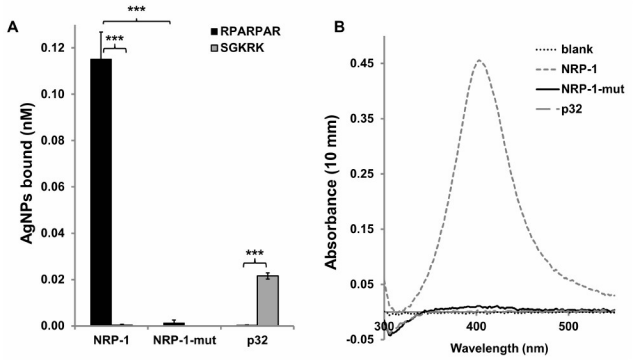

Fig. 2 Binding of peptide particles to receptor proteins. (A) R-AgNPs bind to immobilized NRP1-b1b2 domain but not to NRP1-b1b2 protein with mutated CendR binding pocket[7] or to p32 protein; K-AgNPs bind to p32 and not to wt or mutant NRP1-b1b2. Data represent mean values ± SD (n=3); *** $p < 0.001$ by Student's t-test. (B) Representative raw data from UV-vis spectroscopy for R-AgNPs. AgNPs were eluted from protein-loaded Ni-NTA magnetic beads with 0.4 M imidazole-containing buffer and the UV-vis spectrum of the eluate was measured. The absorbance spectrum seen for NRP-1 binding is due to R-AgNPs; the peak absorbance was taken for calculations.

the CGKRK peptide[12], but not to b1b2. Control B-AgNPs did not bind to either target protein (results not shown).

We next tested cellular binding and internalization of individual AgNPs using two cancer cell lines: PPC-1 prostate carcinoma cells, which express high levels of NRP-1 and some p32, and M21 melanoma cells, which express p32 and are negative for NRP-1 expression (Supp. Figure 2). To facilitate detection by flow cytometry and fluorescence microscopy we labeled the neutravidin AgNP coating with CF555 fluorescent dye prior to loading of biotin or biotin peptides. Binding assays using flow cytometry showed that R-AgNPs were bound and taken up by NRP-1-positive PPC-1 cells, but not by the NRP-1-negative M21 cells (Figure 3A). The PPC-1 and M21 cells in a mixed culture could be phenotypically readily distinguished based on their AgNP uptake pattern: R-AgNPs co-localized with NRP-1 on the surface and in endocytic vesicles of PPC-1 cells, whereas M21 cells remained negative (Figure 3B). In contrast, both cell lines bound K-AgNPs in agreement with the fact that both express p32. Control B-AgNPs showed only background binding in both cells lines. These results show that AgNP tropism could be accurately directed by attaching targeting peptides to the NP surface.

Next, we studied isotopically barcoded AgNPs, doped with palladium or made from different isotopes of silver. To establish a baseline for the ICP-MS-based cellular uptake assay, we studied cellular binding and internalization of our three isotopically-tagged types of AgNPs, functionalized with RPARPAR peptide. Each of the R-AgNPs bound efficiently to PPC-1 cells, and ICP-MS could correctly identify the expected Ag isotopes and Pd doping (Figure 4A). The specificity of the R-AgNPs was demonstrated by their limited binding to M21 cells. These data show that the core type has negligible effect on the functionality of the peptide-AgNPs. Removal of cell surface-bound NPs by etching resulted in decreased ICP-MS signal[16]. For example, in PPC-1 cells incubated with R-107AgNPs, the etched 107Ag signal was 25.7 ± 1.5 ng/g versus 61.0 ± 5.6 ng/g for non-etched cells.

To assess the multiplexing potential of AgNPs, cells were incubated with a cocktail of R-AgNPs, K-AgNPs, and B-AgNPs and internalization of each type of nanoparticle was quantified. Extracellular and non-specifically bound AgNPs were removed by etching and washing (see Methods). ICP-MS analysis showed that, PPC-1 cells contained 75 ± 5% R-AgNPs and 25 ± 2% K-AgNPs (Figure 4B). In M21 cells the ratio was reversed; they contained 11 ± 1% R-AgNPs and 89 ± 9% K-AgNPs (Figure 4B). The preferential uptake of R-AgNPs by PPC-1 cells rather than M21 cells was highly significant: 18.3 ± 1.2 ng/g vs. 1.3 ± 0.2 ng/g, $p < 0.001$. Conversely M21 cells took up more K-AgNPs (10.6 ± 1.1 ng/g) than PPC-1 cells (6.2 ± 0.4 ng/g), $p < 0.01$. Of note, K-AgNP uptake by PPC-1 cells was elevated when these AgNPs were applied to the cells together with R-AgNPs as compared to K-AgNPs applied alone. Also, there was a modest increase in R-AgNP uptake in M21 cells when these NPs were administered together with K-AgNPs (Supp. Figure 3). This may be due to a bystander effect[12,20].

B-wtAg-Pd particles are 1% Pd and contain 107Ag and 109Ag, therefore contribution of the B-wtAg-Pd particles to the total amount of Ag must be accounted for when deconvoluting the ICP-MS signal (described in Methods). In the multiplexed ICP-MS internalization assay, the Pd quantity was below the detection limit of 10 pg/g, indicating a low level of B-AgNP uptake. The limited binding of the control particles was also seen for individually-administered B-wtAg-Pd particles (Supp. Figure 4). The background level of binding that can be expected for the biotin control particles was reduced to the detection limit for Pd by etching of the extracellular AgNPs. This result was expected based on microscopy and flow cytometry data (Figure 3) and suggests low background binding for non-targeted AgNPs.

4 Conclusions

We have built an AgNP-based ratiometric system for homing peptide specificity and validation studies. Homing peptides and other affinity ligands are increasingly used for targeted delivery of various therapeutic, imaging, and theranostic nanoparticle payloads to tumors. The ultrasensitive ICP-MS-based ratiometric phenotyping system developed here can be potentially useful for *in vivo* tumor profiling to identify affinity ligands that are best suited for a precision-guided payload delivery to a given tumor.

Acknowledgements

This work was supported by Susan G. Komen for the Cure Foundation career development award KG110704 (TT), European Research Council Starting Grant (GliomaDDS), a grant from European Regional Development Fund (TT), Wellcome Trust International Fellowship WT095077MA (TT), and Norwegian-Estonian collaboration grant EMP181 (TT), and Cancer Center Support Grant CA CA30199 and grant CA152327 from the National Cancer Institute (ER). The authors thank Rein Laiverik for help with electron microscopy.

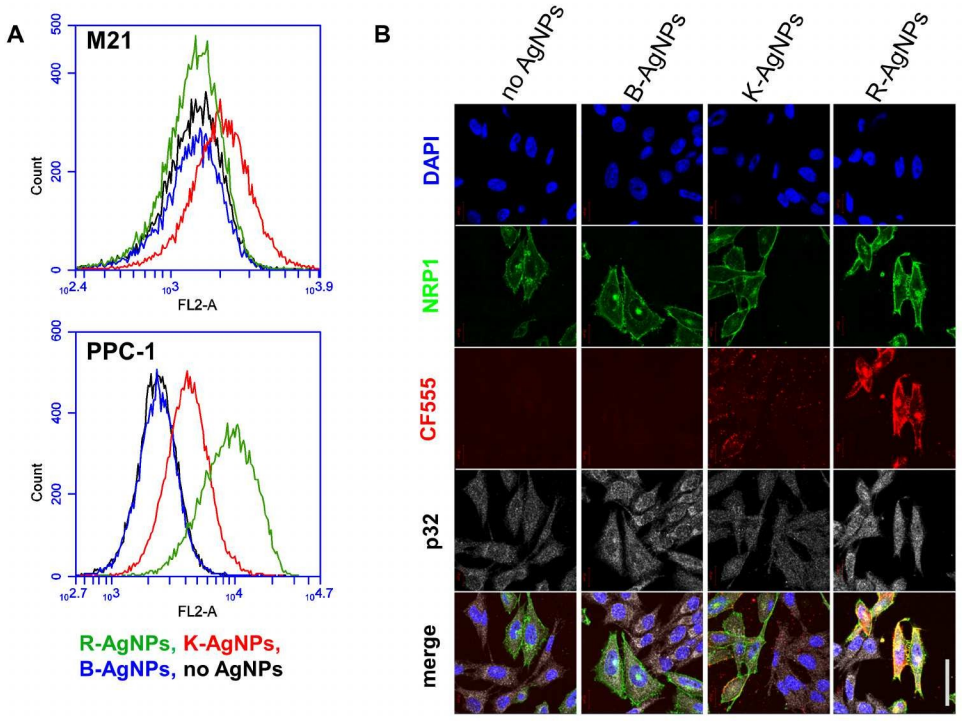

Fig. 3 Receptor-dependent binding and uptake of nanoparticles by PPC-1 and M21 cells. (A) Flow cytometry of M21 and PPC-1 cells incubated for 1 h with R-, K-, or B-AgNPs, all labeled with CF555. Note that NRP-1-positive PPC-1 cells bind R-AgNPs (66 ± 1% positive), whereas M21 do not; both cell lines score positive for binding of K-AgNPs 7 ± 1% positive for M21 and 8 ± 1% for PPC-1 cells (n=3). B) Confocal microscopy pictures of M21 and PPC-1 cells co-cultured as attached cells. The cells can be distinguished by the high cell surface expression of NRP-1 by PPC-1 cells and absence of NRP-1 in M21 cells. AgNPs were labeled with CF555 fluorescent dye. Note cellular uptake of R-AgNPs in NRP-1-positive PPC-1 cells and binding of both PPC-1 and M21 cells by K-AgNPs. Scale bar = 50 μm.

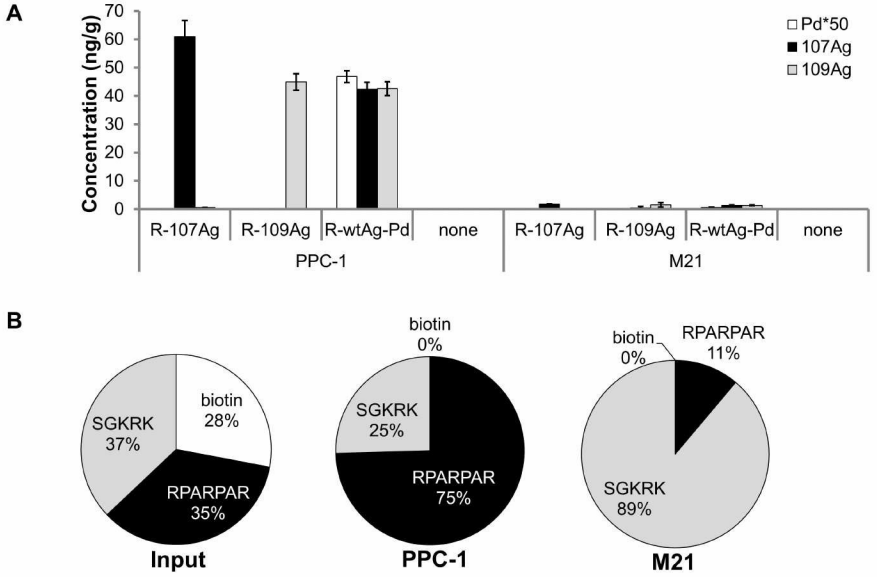

Fig. 4 Isotopic multiplexing of AgNP binding and internalization into M21 and PPC-1 cells. A) Three isotope-tagged RPARPAR-coupled silver cores were incubated with PPC-1 or M21 cells for 1 h and total bound AgNPs were quantified by ICP-MS. Each of the three silver cores functionalized with RPARPAR peptide showed robust PPC-1 binding and low M21 binding. The Pd concentration is multiplied by 50 to visualize more clearly; the R-wt-Ag-Pd sample's Pd content of 0.94 ± 0.04 ng/g is 100 times above the detection limit. Data represent mean values ± SD (n=3). B) Cells incubated with isotopically coded AgNPs (R-107AgNPs, K-109AgNPs, B-wtAg-PdNPs), followed by etching to remove the extracellular nanoparticles and quantification of the internalized nanoparticles by ICP-MS. PPC-1 cells demonstrated preferential uptake of R-AgNPs and M21 cells took up mainly K-AgNPs (n=3).

References

1 M. E. R. O'Brien, N. Wigler, M. Inbar, R. Rosso, E. Grischke, A. Santoro, R. Catane, D. G. Kieback, P. Tomczak, S. P. Ackland, F. Orlandi, L. Mellars, L. Alland and C. Tendler, *Annals of Oncology*, 2004, **15**, 440–449.

2 A. Gabizon, R. Catane, B. Uziely, B. Kaufman, T. Safra, R. Cohen, F. Martin, A. Huang and Y. Barenholz, *Cancer Research*, 1994, **54**, 987–992.

3 M. R. Green, G. M. Manikhas, S. Orlov, B. Afanasyev, A. M. Makhson, P. Bhar and M. J. Hawkins, *Annals of Oncology*, 2006, **17**, 1263–1268.

4 W. J. Gradishar, S. Tjulandin, N. Davidson, H. Shaw, N. Desai, P. Bhar, M. Hawkins and J. O'Shaughnessy, *Journal of Clinical Oncology*, 2005, **23**, 7794–7803.

5 E. Ruoslahti, *Advanced Materials*, 2012, **24**, 3747–3756.

6 F. Fay and C. J. Scott, *Immunotherapy*, 2011, **3**, 381–394.

7 T. Teesalu, K. N. Sugahara, V. R. Kotamraju and E. Ruoslahti, *Proc. Natl. Acad. Sci. USA*, 2009, **106**, 16157–16162.

8 K. N. Sugahara, T. Teesalu, P. P. Karmali, V. R. Kotamraju, L. Agemy, O. M. Girard, D. Hanahan, R. F. Mattrey and E. Ruoslahti, *Cancer Cell*, 2009, **16**, 510–520.

9 B. Chaudhary, Y. Khaled, B. Ammori and E. Elkord, *Cancer Immunology, Immunotherapy*, 2014, **63**, 81 – 99.

10 A. Latil, I. Bièche, S. Pesche, A. Valéri, G. Fournier, O. Cussenot and R. Lidereau, *International Journal of Cancer*, 2000, **89**, 167 – 171.

11 L. Agemy, D. Friedmann-Morvinski, V. R. Kotamraju, L. Roth, K. N. Sugahara, O. M. Girard, R. F. Mattrey, I. M. Verma and E. Ruoslahti, *Proceedings of the National Academy of Sciences*, 2011, **108**, 17450–17455.

12 L. Agemy, V. R. Kotamraju, D. Friedmann-Morvinski, S. Sharma, K. N. Sugahara and E. Ruoslahti, *Mol Ther*, 2013, **21**, 2195–2204.

13 V. Fogal, L. Zhang, S. Krajewski and E. Ruoslahti, *Cancer Research*, 2008, **68**, 7210–7218.

14 R. Amamoto, M. Yagi, Y. Song, Y. Oda, M. Tsuneyoshi, S. Naito, A. Yokomizo, K. Kuroiwa, S. Tokunaga, S. Kato, H. Hiura, T. Samori, D. Kang and T. Uchiumi, *Cancer Science*, 2011, **102**, 639–647.

15 J. A. Hoffman, E. Giraudo, M. Singh, L. Zhang, M. Inoue, K. Porkka, D. Hanahan and E. Ruoslahti, *Cancer Cell*, 2003, **4**, 383 – 391.

16 G. B. Braun, T. Friman, H.-B. Pang, A. Pallaoro, T. H. de Mendoza, A.-M. A. Willmore, V. R. Kotamraju, A. P. Mann, Z.-G. She, K. N. Sugahara, N. O. Reich, T. Teesalu and E. Ruoslahti, *Nature Materials*, 2014, **13**, 904–911.

17 P. C. Lee and D. Meisel, *The Journal of Physical Chemistry*, 1982, **86**, 3391–3395.

18 T. Dadosh, *Materials Letters*, 2009, **63**, 2236 – 2238.

19 Commission on Isotopic Abundances and Atomic Weights, *Isotopic Abundances*, http://www.ciaaw.org/isotopic-abundances.htm.

20 K. N. Sugahara, T. Teesalu, P. P. Karmali, V. R. Kotamraju, L. Agemy, D. R. Greenwald and E. Ruoslahti, *Science*, 2010, **328**, 1031–1035.